Limits on CP-violating hadronic interactions and proton EDM from paramagnetic molecules

V. V. Flambaum[1,2], I. B. Samsonov[1], and H. B. Tran Tan[1]
[1]*School of Physics, University of New South Wales, Sydney 2052, Australia and*
[2]*Helmholtz Institute Mainz, Johannes Gutenberg University, 55099 Mainz, Germany*
(Dated: December 22, 2024)

Experiments with paramagnetic molecules (ThO, HfF^+, YbF, YbOH, BaF, etc.) provide strong constraints on electron electric dipole moment (EDM) and coupling constant C_{SP} of contact semileptonic interaction. We compute contributions to C_{SP} arising from the nucleon EDMs and from the P,T-violating nucleon-nucleon interactions. This allows us to derive limits on the CP-violating parameters, such as the proton EDM, $|d_p| < 4.8\times10^{-25} e\cdot$cm, the QCD vacuum angle, $|\bar\theta| < 7.6\times10^{-10}$, as well as the quark chromo-EDMs and π-meson-nucleon couplings.

arXiv:2004.10359v2 [hep-ph] 29 Apr 2020

Introduction: The Standard Model of elementary particles naturally incorporates the sources for CP (charge and parity) violation represented by the Cabibbo–Kobayashi–Maskawa (CKM) matrix [1, 2] and the QCD vacuum angle [3–5] (see also Refs. [6, 7] and further references therein). While the elements of the CKM matrix are measured to a high accuracy, the exact value of the QCD vacuum angle $\bar\theta$ is not known. In recent years, the precision in modern atomic and molecular EDM experiments has been improved to such a level that constraints on $\bar\theta$ and other CP-violating parameters imposed by these experiments are approaching or even exceeding those of particle physics [8–14]. Experiments with diamagnetic atoms and molecules target the nuclear Schiff moments arising from nucleon EDMs and CP-violating nuclear forces [8, 12, 14–26] whereas those using paramagnetic polar molecules [10, 27–31] aim at measuring the electron EDM.

In paramagnetic atoms, an atomic EDM may be induced by the following contact CP-odd semileptonic operators

$$\mathcal{L} = \frac{G_F}{\sqrt{2}} C^p_{SP}\, \bar e i\gamma_5 e\, \bar p p + \frac{G_F}{\sqrt{2}} C^n_{SP}\, \bar e i\gamma_5 e\, \bar n n\,, \qquad (1)$$

where G_F is the Fermi coupling constant, e, p and n are respectively the electron, proton and neutron fields; C^p_{SP} and C^n_{SP} are the electron couplings to the proton and neutrons, respectively. The subscript SP denotes the nucleon-scalar and electron pseudoscalar two-fermion bilinears.

In polarised polar molecules, the interaction (1) induces shifts of energy levels. The measurement of these shifts places constraints on the value of $C_{SP} \equiv C^p_{SP} Z/A + C^n_{SP} N/A$, where A and Z are the nuclear mass and charge numbers, and $N = A - Z$ is the number of neutrons. The most stringent constraint on C_{SP} is placed by the ACME collaboration [31], which used the molecule ^{232}ThO, (90% C.L.)

$$|C_{SP}|_{\rm Th} < 7.3\times10^{-10}\,. \qquad (2)$$

The coupling constant C_{SP} receives contributions from various CP-violating interactions, including the CP-odd nuclear forces with coupling constants $\xi_{p,n}$ and the nucleon EDM $d_{p,n}$ effects. The parameters $\xi_{p,n}$ and $d_{p,n}$, in turn, may be expressed in terms of more fundamental ones, namely, the π-meson-nucleon coupling constants $\bar g_{0,1,2}$, the quark chromo-EDMs $\tilde d_{d,u}$ and the QCD vacuum angle $\bar\theta$. Our aim is to determine the leading dependence of C_{SP} on the parameters $d_{p,n}$, $\xi_{p,n}$, $\bar g_{0,1,2}$ and $\tilde d_{d,u}$ and $\bar\theta$ for ^{232}Th and several other atoms of experimental interest, including Ba, Yb, Hf, Pb and Ra.

In the recent paper [32], the contributions to C_{SP} from the two-photon and π,η-meson exchanges between electrons and nucleons were calculated. These contributions led to a limit on the QCD vacuum angle $|\bar\theta| \lesssim 3\times10^{-8}$. In this letter, we will take into account nuclear structure effects in the electron-nucleon interaction. As we will demonstrate further, this allows us to find stronger limits on the CP-violating hadronic parameters.

It is important to note that, according to a theorem by Schiff [33], atomic electrons completely shield the atomic nucleus from any constant external electric field, thus diminishing the effects of nuclear EDM. The CP-odd nuclear forces can be measured through the nuclear Schiff moments and magnetic quadrupole moments [34–36], or by means of applying an oscillating electric field and observing nuclear spin rotations as argued in the Refs. [37–41]. However, since the Schiff theorem applies only to a system which interacts electrically, the interaction of the atomic electrons with the magnetic dipole moment of the nucleus allows for a non-zero atomic EDM induced by a nuclear EDM [33]. This letter is devoted to the study of the mechanism for the production of the atomic EDM from the combined electric and magnetic interaction between the atomic electrons and the nucleus.

In Ref. [42] it was argued that for atoms with vanishing nuclear spins there are no non-vanishing contributions to the atomic EDM from CP-violating nuclear scalar polarizability. However, the analysis of Ref. [42] did not take into account specific near-nucleus electronic contributions which are significantly enhanced by relativistic effects in heavy atoms. Indeed, since the electronic s and p Dirac wave functions for a point-like nucleus are singular at the origin, the electronic matrix elements be-

tween these states are formally divergent and thus make significant contributions to the induced atomic EDM. In this letter, we will systematically analyze the contributions to the atomic EDM from such matrix elements in atoms with vanishing nuclear spins and compare them with those arising from the contact electron-nucleon interaction (1). This will allow us to obtain the leading-order dependence $C_{SP}(d_{p,n}, \xi_{p,n}, \bar{g}_{0,1,2}, \tilde{d}_{d,u}, \bar{\theta})$ for several atoms of experimental interest and deduce improved limits on the CP-violating hadronic parameters.

Atomic EDM due to contact electron-nucleon interaction: In an atom, the CP-odd interaction (1) between a valence electron and the nucleus is described by the Hamiltonian $H_c = \frac{G_F}{\sqrt{2}} C_{SP} \gamma_0 \gamma_5 \rho(\mathbf{r})$, where γ_0 and γ_5 are the Dirac matrices, $\mathbf{r}$ is the position vector of the electron and $\rho(\mathbf{r})$ is the normalized nuclear charge density. In the leading approximation, $\rho(\mathbf{r})$ is constant inside the nucleus of radius R_0 and vanishes outside.

The matrix element $\langle p_{1/2}| H_c |s_{1/2}\rangle$ has a large relativistic amplification factor because of the small-distance singularity of the $s_{1/2}$ and $p_{1/2}$ wave functions [43]. As a result, to the leading order, the atomic EDM arising from the interaction H_c may be written as

$$\mathbf{d} \approx 2 \frac{\langle s_{1/2}| e\mathbf{r} |p_{1/2}\rangle \langle p_{1/2}| H_c |s_{1/2}\rangle}{E_{p_{1/2}} - E_{s_{1/2}}}, \quad (3a)$$

$$\langle p_{1/2}| H_c |s_{1/2}\rangle \approx -\frac{G_F}{2\sqrt{2}\pi} \frac{3AZ\alpha\gamma}{2\gamma+1} \frac{c_{s_{1/2}} c_{p_{1/2}} C_{SP}}{R_0^{2-2\gamma}}, \quad (3b)$$

where $E_{s_{1/2}}$ and $E_{p_{1/2}}$ are the energies of the $s_{1/2}$ and $p_{1/2}$ states, respectively; α is the fine structure constant and $\gamma = \sqrt{1 - Z^2\alpha^2}$. Here we have taken into account that for $r \ll a_B/Z$ the $s_{1/2}$ and $p_{1/2}$ Dirac-Coulomb wave functions have the form (see, e.g., Ref. [44])

$$|s_{1/2}\rangle \approx c_{s_{1/2}} r^{\gamma-1} \begin{pmatrix} -(\gamma+1)\Omega_\mu^{-1} \\ iZ\alpha\Omega_\mu^1 \end{pmatrix}, \quad (4a)$$

$$|p_{1/2}\rangle \approx c_{p_{1/2}} r^{\gamma-1} \begin{pmatrix} (1-\gamma)\Omega_\mu^1 \\ iZ\alpha\Omega_\mu^{-1} \end{pmatrix}, \quad (4b)$$

where Ω_μ^κ is the spherical spinor and $c_{s_{1/2}}$, $c_{p_{1/2}}$ are normalization constants. We do not specify the values of these normalization constants, as our final results will be independent of $c_{s_{1/2}}$ and $c_{p_{1/2}}$.

Contribution to the atomic EDM from nucleon permanent EDM: Let $\mathbf{d}_\tau = d_\tau \boldsymbol{\sigma}$ and $\boldsymbol{\mu}_\tau = \mu_0(g_\tau^l \mathbf{l} + g_\tau^s \mathbf{s})$ be the operators of electric and magnetic dipole moments of the nucleon. Here $d_\tau = (d_p, d_n)$ is the nucleon permanent EDM, μ_0 is the nuclear magneton, g_τ^l and g_τ^s are the orbital and spin g-factors of the nucleon. The operators $\mathbf{d}_\tau$ and $\boldsymbol{\mu}_\tau$ couple with the electric and magnetic fields of the electron, yielding the interaction Hamiltonian

$$H = H_E + H_B, \quad H_E = -\frac{e\,\mathbf{d}_\tau \cdot \mathbf{r}}{r^3}, \quad H_B = -\frac{e\,\boldsymbol{\mu}_\tau \cdot (\mathbf{r} \times \boldsymbol{\alpha})}{r^3}, \quad (5)$$

where $\boldsymbol{\alpha}$ are the electron's Dirac matrices.

The unperturbed atomic states will be denoted by $|mm'\rangle = |m\rangle|m'\rangle$, where $|m\rangle$ and $|m'\rangle$ are electronic and nuclear states, respectively. The first-order contributions to the atomic EDM due to the interaction Hamiltonian (5) vanish for spinless nuclei which we consider in this letter, $\langle 0'|\mathbf{s}|0'\rangle = 0$. non-vanishing contributions to the atomic EDM arise in the second order of the perturbation theory (see Ref. [42] for details),

$$\mathbf{d} = 2 \sum_{m,n,n'} \frac{\langle 0| e\mathbf{r} |m\rangle \langle 0'm| H |nn'\rangle \langle n'n| H |00'\rangle}{(E_m - E_0)(E_{00'} - E_{nn'})}, \quad (6)$$

where the sum is taken over $m \neq 0$ and $nn' \neq 00'$. Note also that we employ the notation $E_{nn'} \equiv E_n + E_{n'}$, where E_n and $E_{n'}$ are energies of electronic and nuclear excitations, respectively.

Similarly to the contact interaction considered in the previous section, the expression (6) receives leading contributions from terms with $|0\rangle = |s_{1/2}\rangle$ and $|m\rangle = |p_{1/2}\rangle$. As a result, Eq. (6) may be cast in the form (3a), with the contact interaction operator H_c replaced with an effective interaction Hamiltonian $H_{\rm eff}$ defined by

$$H_{\rm eff} \equiv \sum_{nn' \neq 00'} \frac{|m\rangle \langle 0'm| H |nn'\rangle \langle n'n| H |00'\rangle \langle 0|}{E_{00'} - E_{nn'}}. \quad (7)$$

Upon substitution of the operators (5) into Eq. (7), the contribution to the matrix element of $H_{\rm eff}$ which is linear in $\mathbf{d}_\tau$ may be written as

$$\langle p_{1/2}| H_{\rm eff} |s_{1/2}\rangle = \sum_{n' \neq 0'} \beta_{n'} M(E_{n'}), \quad (8)$$

where $\beta_{n'}$ accounts for the nuclear matrix elements,

$$\beta_{n'} = \langle 0'| \mathbf{d}_\tau |n'\rangle \langle n'| \boldsymbol{\mu}_\tau |0'\rangle, \quad (9)$$

and the function $M(E_{n'})$ represents the contributions due to the electronic matrix elements,

$$M(E_{n'}) = \frac{1}{3} \sum_n \frac{\langle p_{1/2}| \frac{e\mathbf{r}}{r^3} |n\rangle \langle n| \frac{e(\mathbf{r}\times\boldsymbol{\alpha})}{r^3} |s_{1/2}\rangle}{E_{s_{1/2}0'} - E_{nn'}} + \frac{1}{3} \sum_n \frac{\langle p_{1/2}| \frac{e(\mathbf{r}\times\boldsymbol{\alpha})}{r^3} |n\rangle \langle n| \frac{e\mathbf{r}}{r^3} |s_{1/2}\rangle}{E_{s_{1/2}0'} - E_{nn'}}. \quad (10)$$

For each nuclear energy $E_{n'}$, the value of the function $M(E_{n'})$ is calculated numerically using the method described, e.g., in Ref. [43]. Within this method, one first solves for the corrections to the wave function $|s_{1/2}\rangle$ due to the perturbations $e(\mathbf{r} \times \boldsymbol{\alpha})/r^3$ and $\mathbf{r}/r^3$, respectively, and then integrates with the $|p_{1/2}\rangle$ wave function. Further details of these computations are given in Appendix B.

The nuclear matrix elements (9) correspond to the spin-flip M1 nuclear transitions. The computations of

these matrix elements slightly differ for spherical and deformed nuclei. For the former, it is appropriate to describe the nuclear states in the spherical basis, in which the matrix elements of the total momentum $\mathbf{j}$ vanish for fine structure doublets. As a result, substituting the operators $\mathbf{d}_\tau$ and $\boldsymbol{\mu}_\tau$ into Eq. (9) and using the identity $\mathbf{l} = \mathbf{j} - \mathbf{s}$, the nuclear matrix elements may be written as $\langle 0'|\mathbf{d}_\tau|n'\rangle\langle n'|\boldsymbol{\mu}_\tau|0'\rangle = 2\mu_0 d_\tau(g^s_\tau - g^l_\tau)|\langle n'|\mathbf{s}|0'\rangle|^2$. For deformed nuclei, the states are usually represented within the Nilsson basis [45], in which $\langle 0'|\,\mathbf{l}\,|n'\rangle\,\langle n'|\,\mathbf{s}\,|0'\rangle = 0$. Thus, for deformed nuclei in Eq. (9) we have $\langle 0'|\mathbf{d}_\tau|n'\rangle\langle n'|\boldsymbol{\mu}_\tau|0'\rangle = 2\mu_0 d_\tau g^s_\tau|\langle n'|\mathbf{s}|0'\rangle|^2$. These two cases may be combined in one expression

$$\beta_{n'} = 2d_\tau\mu_0\left(g^s_\tau - \epsilon g^l_\tau\right)|\,\langle 0'|\,\mathbf{s}\,|n'\rangle\,|^2\,, \tag{11}$$

where $\epsilon = 1$ for spherical nuclei and $\epsilon = 0$ for deformed ones.

In Eq. (11), the values of the g-factors for the proton and neutron are $g^l_p = 1$, $g^s_p = 5.586$, $g^l_n = 0$ and $g^s_n = -3.826$, respectively. The energies $E_{n'}$ and matrix elements $\langle 0'|\,\mathbf{s}\,|n'\rangle$ of the spin-flip M1 transitions are listed in Appendix A for different nuclei of interest.

It is convenient to denote the energies and matrix elements for proton M1 spin-flip transitions as E_π and $\langle 0'|\,\mathbf{s}\,|n'\rangle_\pi$, and for neutron transitions as E_ν and $\langle 0'|\,\mathbf{s}\,|n'\rangle_\nu$. With $\beta_{n'}$ given by Eq. (11), this allows us to represent the matrix element (8) in a compact form

$$\langle p_{1/2}|H_{\rm eff}|s_{1/2}\rangle = 2\mu_0\sum_{\tau=p,n} d_\tau\left(g^s_\tau - \epsilon g^l_\tau\right)M_\tau\,, \tag{12}$$

where the quantities M_p and M_n are defined by

$$M_{p(n)} \equiv \sum_{E_{\pi(\nu)}}|\,\langle 0'|\,\mathbf{s}\,|n'\rangle_{\pi(\nu)}\,|^2 M(E_{\pi(\nu)})\,. \tag{13}$$

Note that for deformed nuclei this expression simplifies, because in the Nilsson basis $|\,\langle 0'|\,\mathbf{s}\,|n'\rangle\,|^2 = 1$.

The details of numerical computations of the coefficients M_p and M_n are given in Appendix B. In particular, for ^{232}Th they are $M_p = 0.053 c_{s_{1/2}}c_{p_{1/2}}\mathrm{fm}^{-3}$ and $M_n = 0.12 c_{s_{1/2}}c_{p_{1/2}}\mathrm{fm}^{-3}$. For ^{180}Hf, $M_p = 0.2 c_{s_{1/2}}c_{p_{1/2}}\mathrm{fm}^{-3}$ and $M_n = 0.12 c_{s_{1/2}}c_{p_{1/2}}\mathrm{fm}^{-3}$.

Contributions to the atomic EDM from P,T-odd nuclear forces: The P,T-odd nucleon-nucleon interaction may be effectively taken into account by introducing the perturbed nuclear wave functions [34]

$$|n'\rangle \to |\tilde{n}'\rangle = (1 + \xi_\tau\boldsymbol{\sigma}\cdot\nabla)\,|n'\rangle\,, \tag{14}$$

where $\xi_\tau = (\xi_p, \xi_n)$ is the effective coupling constant. This P,T-odd nucleon-nucleon interaction amounts to the atomic EDM which arises due to the interaction Hamiltonian (5), with $\mathbf{d}_\tau = e_\tau\mathbf{r}$ being the nuclear electric dipole operator. Here $e_\tau = (e_p, e_n)$ is the effective charge of the nucleon, $e_p = (N/A)e$, $e_n = -(Z/A)e$, which appears due to the recoil effect.

The leading contribution to the atomic EDM may be represented by an equation similar to (3a), in which the Hamiltonian H_c is replaced with the effective Hamiltonian (7) possessing the matrix element of the form (8). The only new feature is that the nuclear matrix elements (9) are now given by $\beta_{n'} = \langle\tilde{0}'|\mathbf{d}_\tau|\tilde{n}'\rangle\langle\tilde{n}'|\boldsymbol{\mu}_\tau|\tilde{0}'\rangle$. Substituting here the P,T-perturbed nuclear states (14) and taking into account the comments above Eq. (11), we find

$$\begin{aligned}\beta_{n'} = &-2\mu_0 e_\tau\xi_\tau\left(g^s_\tau - \epsilon g^l_\tau\right)|\langle 0'|\mathbf{s}|n'\rangle|^2 \\ &+ 2\mu_0 e_\tau\xi_\tau\left(g^s_\tau - g^l_\tau\right)\langle 0'|\mathbf{r}|n'\rangle\langle n'|\mathbf{s}\times\mathbf{p}|0'\rangle\,,\end{aligned} \tag{15}$$

where $\mathbf{p}$ is the nucleon momentum operator.

The last term in Eq. (15) involves the E1 matrix element $\langle 0'|\mathbf{r}|n'\rangle$ which may be accounted for within the giant resonance model. In this model, we assume that all the E1 matrix elements have approximately the same energy $\bar{E}$, which is the energy of the E1 giant resonance. In this case, after the summation over n', the last term in Eq. (15) is proportional to $\sum_{n'}\langle 0'|\mathbf{r}|n'\rangle\langle n'|\mathbf{s}\times\mathbf{p}|0'\rangle = -\langle 0'|\mathbf{l}\cdot\mathbf{s}|0'\rangle \equiv -\langle\mathbf{l}\cdot\mathbf{s}\rangle$, where we have taken into account the completeness of the states $|n'\rangle$. The expectation value of the $\mathbf{l}\cdot\mathbf{s}$ operator may be estimated using Nilsson nuclear model [45, 46]. The values of these matrix elements as well as the energies $\bar{E}$ are listed for different nuclei of interest in Appendix A.

Taking into account the above comments about the nuclear matrix elements, one may substitute the expression (15) into Eq. (8) and find the matrix element of the effective interaction Hamiltonian

$$\begin{aligned}\langle s_{1/2}|H_{\rm eff}|p_{1/2}\rangle = -2\mu_0\sum_{\tau=p,n} e_\tau\xi_\tau\Big[&(g^s_\tau - \epsilon g^l_\tau)M_\tau \\ &+ (g^s_\tau - g^l_\tau)\langle\mathbf{l}\cdot\mathbf{s}\rangle_\tau M(\bar{E})\Big]\,,\end{aligned} \tag{16}$$

where $\langle\mathbf{l}\cdot\mathbf{s}\rangle_p$ and $\langle\mathbf{l}\cdot\mathbf{s}\rangle_n$ are expectation values of the $\mathbf{l}\cdot\mathbf{s}$ operator for the proton and neutron states, respectively.

The values of the coefficients M_p and M_n for ^{232}Th and ^{180}Hf were given at the end of the previous section. For the coefficient $M(\bar{E})$ we find: For ^{232}Th, $M(\bar{E}) = 4.1\times10^{-4}c_{s_{1/2}}c_{p_{1/2}}\mathrm{fm}^{-3}$ and for ^{180}Hf, $M(\bar{E}) = 1.9\times10^{-3}c_{s_{1/2}}c_{p_{1/2}}\mathrm{fm}^{-3}$, see Table III in Appendix B.

Constraints on CP-odd hadronic parameters: In Eqs. (12) and (16), we computed the contributions to the atomic EDM (3a) due to the nucleon EDMs and P,T-odd nuclear interactions. It is natural to compare these contributions with that due to the contact interaction H_c. This amounts to comparing the sum of the matrix elements (12) and (16) with the matrix element (3b). Equating these matrix elements gives the following relation between the constant C_{SP} and the parameters d_p, d_n and ξ_p, ξ_n:

$$C_{SP} = -\frac{4\sqrt{2}\pi}{G_F}\frac{2\gamma+1}{3AZ\alpha\gamma}\frac{\mu_0 R_0^{2\gamma-2}}{c_{s_{1/2}}c_{p_{1/2}}}\sum_{\tau=p,n}\left[(g_\tau^s-\epsilon g_\tau^l)M_\tau\left(d_\tau-e_\tau\xi_\tau\right)-(g_\tau^s-g_\tau^l)M(\bar{E})e_\tau\xi_\tau\langle\mathbf{l}\cdot\mathbf{s}\rangle_\tau\right]. \quad (17)$$

We point out that the right-hand side of Eq. (17) is independent of the wave functions normalization constants $c_{s_{1/2}}$ and $c_{p_{1/2}}$. Indeed, as is seen from the definition (10), the function $M(E)$ contains the same normalization constants, so that they cancel out in Eqs. (17).

Taking into account the numerical values of all parameters, Eq. (17) may be cast in the final form

$$C_{SP} = (\lambda_1 d_p - \lambda_2 d_n - \lambda_3 e\xi_p - \lambda_4 e\xi_n)\times\frac{10^{15}}{e\cdot\mathrm{cm}}, \quad (18)$$

where the values of the coefficients $\lambda_1,\ldots,\lambda_4$ for several atoms of interest are presented in Table I.

The relations (17) and (18) represent the central results of this letter. They allow us to place limits on the nucleon EDMs d_τ and the coupling constants of P,T-odd nuclear forces ξ_τ. Taking into account the most recent constraint on $|C_{SP}|$ from the HfF^+ [29] and ThO [31] EDM experiments (see also Ref. [47]), we obtain the limits on $|d_p|$ and $|\xi_{p,n}|$. These results are collected in Table II.

Eq. (17) may be used to place limits on other hadronic CP-violating parameters, such as the quark chromo-EDMs $\tilde{d}_{d,u}$, the π-meson-nucleon interaction constants $\bar{g}_{0,1,2}$ and the QCD vacuum angle $\bar{\theta}$. These parameters are related to d_τ and ξ_τ as follows [34, 48–52] (see also Refs. [6, 7]): $d_p = 1.1e(0.5\tilde{d}_d+\tilde{d}_u)$, $d_n = 1.1e(\tilde{d}_d+0.5\tilde{d}_u)$, $d_p = 2.1\times10^{-16}\bar{\theta}e\cdot\mathrm{cm}$, $d_n = -2.7\times10^{-16}\bar{\theta}e\cdot\mathrm{cm}$, $\xi_p = -\xi_n = 7.4\times10^{-16}\bar{\theta}\mathrm{cm}$, $\xi_p = -\xi_n = 10^{-14}g\left(-0.2\bar{g}_0+\bar{g}_1+0.42\bar{g}_2\right)\mathrm{cm}$, $g\bar{g}_0 = 0.21\bar{\theta}$, $g\bar{g}_0 = 0.8\times10^{15}(\tilde{d}_u+\tilde{d}_d)\mathrm{cm}^{-1}$, $g\bar{g}_1 = -0.046\bar{\theta}$ and $g\bar{g}_1 = 4.0\times10^{15}(\tilde{d}_u-\tilde{d}_d)\mathrm{cm}^{-1}$. Using these relations and Eq. (18), we find:

$$C_{SP} = -\lambda_5\left(-0.20g\bar{g}_0+g\bar{g}_1+0.42g\bar{g}_2\right), \quad (19a)$$
$$C_{SP} = (\lambda_6\tilde{d}_d-\lambda_7\tilde{d}_u)\times10^{15}\mathrm{cm}^{-1}, \quad (19b)$$
$$C_{SP} = \lambda_8\bar{\theta}, \quad (19c)$$

where the numerical values of the coefficients $\lambda_5,\ldots,\lambda_8$ are given in Table I. The limits on $\bar{g}_i$, $\tilde{d}_{d,u}$ and $\bar{\theta}$ which follow from Eqs. (19) are presented in Table II.

		λ_1	λ_2	λ_3	λ_4	λ_5	λ_6	λ_7	λ_8
Spherical	^{138}Ba	1.26	1.01	1.03	0.75	2.75	11.0	9.73	0.33
	^{206}Pb	0.92	1.51	0.84	0.84	0.04	-1.02	-0.04	0.60
	^{208}Pb	0.91	0.55	0.84	0.44	4.01	16.6	14.7	0.04
Deformed	^{172}Yb	2.52	1.93	1.79	1.04	7.50	30.4	27.1	0.49
	^{174}Yb	2.48	2.89	1.78	1.45	3.34	12.1	11.7	1.05
	^{176}Yb	2.45	2.42	1.77	1.17	5.99	23.6	21.6	0.72
	^{178}Hf	6.53	2.20	4.15	1.10	30.4	128	111	-0.29
	^{180}Hf	6.43	2.45	4.11	1.25	28.6	120	104	-0.11
	^{226}Ra	1.11	0.84	0.80	0.41	3.87	15.8	14.1	0.17
	^{232}Th	1.54	2.41	1.02	0.99	0.24	-0.81	0.56	0.95

Table I: The results of numerical computations of the coefficients $\lambda_1,\ldots,\lambda_8$ in Eqs. (18) and (19).

	$^{180}HfF^+$	^{232}ThO
$\lvert C_{SP}\rvert$	1.8×10^{-8} [29, 47]	7.3×10^{-10} [31]
$\lvert d_p\rvert$	$2.8\times10^{-24}e\cdot\mathrm{cm}$	$4.8\times10^{-25}e\cdot\mathrm{cm}$
$\lvert\xi_p\rvert$	$5.1\times10^{-23}\mathrm{cm}$	$8.4\times10^{-24}\mathrm{cm}$
$\lvert\xi_n\rvert$	$1.7\times10^{-22}\mathrm{cm}$	$8.6\times10^{-24}\mathrm{cm}$
$\lvert\bar{g}_0\rvert$	2.3×10^{-10}	1.1×10^{-9}
$\lvert\bar{g}_1\rvert$	4.6×10^{-11}	2.2×10^{-10}
$\lvert\bar{g}_2\rvert$	1.1×10^{-10}	5.3×10^{-10}
$\lvert\tilde{d}_u\rvert$	$1.7\times10^{-25}\mathrm{cm}$	$1.3\times10^{-24}\mathrm{cm}$
$\lvert\tilde{d}_d\rvert$	$1.5\times10^{-25}\mathrm{cm}$	$9.1\times10^{-25}\mathrm{cm}$
$\lvert\bar{\theta}\rvert$	1.7×10^{-7}	7.6×10^{-10}

Table II: Limits on absolute values of CP-violating hadronic parameters arising from the relations (18) and (19) upon implementing the constraints on the constant C_{SP} from the $^{180}HfF^+$ [29, 47] and ^{232}ThO [31] experiments.

Conclusions: In this letter, we demonstrated that the experiments measuring the electron electric dipole moment (eEDM) with paramagnetic atoms and molecules are also sensitive to the nucleon EDMs and P,T-violating nucleon-nucleon interactions. Dominant contributions to the atomic EDM in such atoms arise from the combined electric and magnetic electron-nucleus interaction. Taking into account nuclear structure effects, we derived relations between the electron-nucleus contact interaction constant C_{SP} and CP-violating parameters. Using the limit on C_{SP} from ThO experiment [31], we placed independent limits on the proton EDM, $|d_p| < 4.8\times10^{-25}e\cdot$cm, and the QCD vacuum angle, $|\bar{\theta}| < 7.6\times10^{-10}$, and other CP-odd parameters. We expect that the obtained relations may place the most stringent limits on these parameters once improved constraints on C_{SP} are available from next generations of eEDM experiments [10, 11, 29–31, 53].

Acknowledgements: This work was supported

by the Australian Research Council Grant No. DP150101405 and the Gutenberg Fellowship. We thank Vladimir Dmitriev and Anna Viatkina for useful discussions.

Appendix A: Nuclear energies and matrix elements

In this appendix, we estimate the nuclear matrix elements and corresponding energies of M1 spin-flip nuclear single-particle transitions. The details of these computations slightly differ for (nearly) spherical and deformed nuclei. Therefore, we consider these two cases separately.

Spherical nuclei

In this section, we focus on the ^{208}Pb, ^{206}Pb and ^{138}Ba nuclei, which are nearly spherical, i.e., they have deformation $\delta < 0.1$. For such a nucleus, proton and neutron single-particle states may be labeled as $|n, l, j, m\rangle$, where n is the oscillator quantum number, l and j are the orbital and total momentum numbers, m is magnetic quantum number. In this basis, the nuclear spin operator $\mathbf{s}$ provides transitions between fine structure doublets.

In the ^{208}Pb nucleus, the non-vanishing matrix elements of the spin operator are $\langle 5h\frac{9}{2}|\mathbf{s}|5h\frac{11}{2}\rangle$ for protons and $\langle 6i\frac{11}{2}|\mathbf{s}|6i\frac{13}{2}\rangle$ for neutrons. The isotope ^{206}Pb has additional contributions from the $\langle 5p\frac{1}{2}|\mathbf{s}|5p\frac{3}{2}\rangle$ neutron matrix elements. For ^{138}Ba, non-vanishing proton contributions arise from the matrix elements $\langle 4d\frac{3}{2}|\mathbf{s}|4d\frac{5}{2}\rangle$ and $\langle 4g\frac{9}{2}|\mathbf{s}|4g\frac{7}{2}\rangle$ whereas neutron contributions come from $\langle 5h\frac{9}{2}|\mathbf{s}|5h\frac{11}{2}\rangle$. All these matrix elements are calculated using the properties of spherical spinors (see, e.g., Ref. [54]). The energies of all these transitions are estimated with the use of Fig. 5 in Ref. [46]. When the energies are (nearly) degenerate, we give the sum of matrix elements corresponding to the same energy. In the tables below, we collect the values of such matrix elements with the corresponding energies for ^{208}Pb, ^{206}Pb and ^{138}Ba. These tables also include the expectation values of the $\mathbf{l}\cdot\mathbf{s}$ operator and the energies of the giant electric dipole resonance estimated by the empirical formula $\bar{E} = 95(1 - A^{-1/3})A^{-1/3}$ MeV, with A being the mass number of a heavy nucleus [55, 56].

^{138}Ba

Proton transitions		Neutron transitions	
$\lvert\langle n'\lvert\mathbf{s}\rvert 0'\rangle_p\rvert^2$	$E_{n'}$ (MeV)	$\lvert\langle n'\lvert\mathbf{s}\rvert 0\rangle'_n\rvert^2$	$E_{n'}$ (MeV)
$\frac{18}{25}$	2.7	$\frac{170}{121}$	5.3
$\frac{2}{25}$	4.1	$\frac{200}{121}$	5.4
$\frac{28}{81}$	4.3	$\frac{30}{121}$	5.5
$\frac{56}{81}$	4.4	$\frac{136}{121}$	5.9
$\frac{16}{81}$	4.5	$\frac{56}{121}$	6.0
$\frac{8}{9}$	4.6	$\frac{60}{121}$	6.2
$\frac{8}{81}$	5.2	$\frac{8}{121}$	6.5
$\langle 0'\lvert\mathbf{l}\cdot\mathbf{s}\rvert 0'\rangle_p = 7$		$\langle 0'\lvert\mathbf{l}\cdot\mathbf{s}\rvert 0'\rangle_n = 15$	
$\bar{E} = 14.8$ MeV, $\delta = 0.09$			

^{208}Pb

Proton transitions		Neutron transitions	
$\lvert\langle n'\lvert\mathbf{s}\rvert 0'\rangle_p\rvert^2$	$E_{n'}$ (MeV)	$\lvert\langle n'\lvert\mathbf{s}\rvert 0\rangle'_n\rvert^2$	$E_{n'}$ (MeV)
$\frac{10}{11}$	4.5	$\frac{72}{169}$	6.1
$\frac{162}{121}$	4.6	$\frac{462}{169}$	6.2
$\frac{98}{121}$	4.7	$\frac{318}{169}$	6.3
$\frac{250}{121}$	4.8	$\frac{132}{169}$	6.4
$\frac{32}{121}$	5.0	$\frac{100}{169}$	6.5
$\frac{8}{121}$	5.1	$\frac{6}{169}$	6.7
		$\frac{2}{169}$	6.9
$\langle 0'\lvert\mathbf{l}\cdot\mathbf{s}\rvert 0'\rangle_p = 15$		$\langle 0'\lvert\mathbf{l}\cdot\mathbf{s}\rvert 0'\rangle_n = 21$	
$\bar{E} = 13.3$ MeV, $\delta = 0.05$			

^{206}Pb

Proton transitions		Neutron transitions	
$\lvert\langle n'\lvert\mathbf{s}\rvert 0'\rangle_p\rvert^2$	$E_{n'}$ (MeV)	$\lvert\langle n'\lvert\mathbf{s}\rvert 0\rangle'_n\rvert^2$	$E_{n'}$ (MeV)
$\frac{10}{11}$	4.5	$\frac{72}{169}$	6.1
$\frac{162}{121}$	4.6	$\frac{462}{169}$	6.2
$\frac{98}{121}$	4.7	$\frac{318}{169}$	6.3
$\frac{250}{121}$	4.8	$\frac{132}{169}$	6.4
$\frac{32}{121}$	5.0	$\frac{100}{169}$	6.5
$\frac{8}{121}$	5.1	$\frac{6}{169}$	6.7
		$\frac{2}{169}$	6.9
		$\frac{2}{3}$	1.4
		$\frac{10}{9}$	2.0
$\langle 0'\lvert\mathbf{l}\cdot\mathbf{s}\rvert 0'\rangle_p = 15$		$\langle 0'\lvert\mathbf{l}\cdot\mathbf{s}\rvert 0'\rangle_n = 21$	
$\bar{E} = 13.3$ MeV, $\delta = 0.03$			

Deformed nuclei

For deformed heavy nuclei with $\delta > 0.1$, it is convenient to use the Nilsson basis [45, 46]. In this basis, proton and neutron single-particle states are labeled as $|n_3, n_\perp, \Lambda, \Omega\rangle$, where n_3 and $n_\perp$ are the oscillator quantum numbers, Λ and Ω are the projections of angular and total momenta on the deformation axis. Note that $\Omega = \Lambda + \Sigma$ where Σ is the projection of the nucleon's spin

on the deformation axis. The dependence of the energy levels on the deformation parameter δ in this model is represented in Fig. 5 in Ref. [46]. From such dependence, one may estimate the energies of the spin-flip transitions. Note that in the basis $|n_3, n_\perp, \Lambda, \Omega\rangle$ each spin-flip M1 matrix element is $\langle m'|\, s_+ \,|0'\rangle = 1$, and the corresponding energy level is doubly degenerate since each quantum number Σ corresponds to $\pm\Lambda$.

One may also compute the ground state expectation value $\langle 0'|\, \mathbf{l}\cdot\mathbf{s}\,|0'\rangle = \langle 0'|\, \Lambda\Sigma\,|0'\rangle$ with the corresponding energies by taking the sum over Λ and Σ quantum numbers for all protons and neutron, respectively, $\langle 0'|\mathbf{l}\cdot\mathbf{s}|0'\rangle_{p,n} = \sum_{p,n} \Lambda\cdot\Sigma$.

The values of the single-nucleon spin-flip transition energies, the ground state expectation values $\langle 0'|\, \mathbf{l}\cdot\mathbf{s}\,|0'\rangle$, the electric dipole giant resonance energies and the deformation parameter δ for several nuclei of interest are presented in the corresponding tables below.

^{172}Yb

Proton transitions		Neutron transitions	
Transition	$E_{n'}$ (MeV)	Transition	$E_{n'}$ (MeV)
$\|523\frac{7}{2}\rangle \to \|\frac{5}{2}\rangle$	4.5	$\|651\frac{3}{2}\rangle \to \|\frac{1}{2}\rangle$	3.9
$\|532\frac{5}{2}\rangle \to \|\frac{3}{2}\rangle$	4.0	$\|642\frac{5}{2}\rangle \to \|\frac{3}{2}\rangle$	4.5
$\|541\frac{3}{2}\rangle \to \|\frac{1}{2}\rangle$	4.5	$\|633\frac{7}{2}\rangle \to \|\frac{5}{2}\rangle$	5.0
$\|404\frac{9}{2}\rangle \to \|\frac{7}{2}\rangle$	4.1	$\|505\frac{11}{2}\rangle \to \|\frac{9}{2}\rangle$	5.1
		$\|514\frac{9}{2}\rangle \to \|\frac{7}{2}\rangle$	4.6
$\langle 0'\|\mathbf{l}\cdot\mathbf{s}\|0'\rangle = 10$		$\langle 0'\|\mathbf{l}\cdot\mathbf{s}\|0'\rangle = 15$	
$\bar{E} = 14.0$ MeV, $\delta = 0.31$			

^{174}Yb

Proton transitions		Neutron transitions	
Transition	$E_{n'}$ (MeV)	Transition	$E_{n'}$ (MeV)
$\|523\frac{7}{2}\rangle \to \|\frac{5}{2}\rangle$	4.5	$\|651\frac{3}{2}\rangle \to \|\frac{1}{2}\rangle$	3.9
$\|532\frac{5}{2}\rangle \to \|\frac{3}{2}\rangle$	4.0	$\|642\frac{5}{2}\rangle \to \|\frac{3}{2}\rangle$	4.5
$\|541\frac{3}{2}\rangle \to \|\frac{1}{2}\rangle$	4.5	$\|633\frac{7}{2}\rangle \to \|\frac{5}{2}\rangle$	5.0
$\|404\frac{9}{2}\rangle \to \|\frac{7}{2}\rangle$	4.1	$\|505\frac{11}{2}\rangle \to \|\frac{9}{2}\rangle$	5.1
		$\|514\frac{9}{2}\rangle \to \|\frac{7}{2}\rangle$	4.6
		$\|512\frac{5}{2}\rangle \to \|\frac{3}{2}\rangle$	2.4
$\langle 0'\|\mathbf{l}\cdot\mathbf{s}\|0'\rangle = 10$		$\langle 0'\|\mathbf{l}\cdot\mathbf{s}\|0'\rangle = 17$	
$\bar{E} = 14.0$ MeV, $\delta = 0.31$			

^{176}Yb

Proton transitions		Neutron transitions	
Transition	$E_{n'}$ (MeV)	Transition	$E_{n'}$ (MeV)
$\|523\frac{7}{2}\rangle \to \|\frac{5}{2}\rangle$	4.5	$\|651\frac{3}{2}\rangle \to \|\frac{1}{2}\rangle$	4.2
$\|532\frac{5}{2}\rangle \to \|\frac{3}{2}\rangle$	4.1	$\|642\frac{5}{2}\rangle \to \|\frac{3}{2}\rangle$	4.5
$\|541\frac{3}{2}\rangle \to \|\frac{1}{2}\rangle$	4.5	$\|633\frac{7}{2}\rangle \to \|\frac{5}{2}\rangle$	5.0
$\|404\frac{9}{2}\rangle \to \|\frac{7}{2}\rangle$	4.0	$\|505\frac{11}{2}\rangle \to \|\frac{9}{2}\rangle$	5.2
		$\|512\frac{5}{2}\rangle \to \|\frac{3}{2}\rangle$	2.4
$\langle 0'\|\mathbf{l}\cdot\mathbf{s}\|0'\rangle = 10$		$\langle 0'\|\mathbf{l}\cdot\mathbf{s}\|0'\rangle = 13$	
$\bar{E} = 13.9$ MeV, $\delta = 0.29$			

^{178}Hf

Proton transitions		Neutron transitions	
Transition	$E_{n'}$ (MeV)	Transition	$E_{n'}$ (MeV)
$\|523\frac{7}{2}\rangle \to \|\frac{5}{2}\rangle$	4.4	$\|505\frac{11}{2}\rangle \to \|\frac{9}{2}\rangle$	4.2
$\|532\frac{5}{2}\rangle \to \|\frac{3}{2}\rangle$	4.1	$\|512\frac{5}{2}\rangle \to \|\frac{3}{2}\rangle$	2.4
$\|541\frac{3}{2}\rangle \to \|\frac{1}{2}\rangle$	4.1	$\|633\frac{7}{2}\rangle \to \|\frac{5}{2}\rangle$	5.0
$\|402\frac{5}{2}\rangle \to \|\frac{3}{2}\rangle$	1.9	$\|642\frac{5}{2}\rangle \to \|\frac{3}{2}\rangle$	4.6
$\|411\frac{3}{2}\rangle \to \|\frac{1}{2}\rangle$	1.4	$\|631\frac{3}{2}\rangle \to \|\frac{1}{2}\rangle$	7.8
$\langle 0'\|\mathbf{l}\cdot\mathbf{s}\|0'\rangle = 9$		$\langle 0'\|\mathbf{l}\cdot\mathbf{s}\|0'\rangle = 17$	
$\bar{E} = 13.8$ MeV, $\delta = 0.26$			

^{180}Hf

Proton transitions		Neutron transitions	
Transition	$E_{n'}$ (MeV)	Transition	$E_{n'}$ (MeV)
$\|523\frac{7}{2}\rangle \to \|\frac{5}{2}\rangle$	4.4	$\|505\frac{11}{2}\rangle \to \|\frac{9}{2}\rangle$	4.2
$\|532\frac{5}{2}\rangle \to \|\frac{3}{2}\rangle$	4.1	$\|512\frac{5}{2}\rangle \to \|\frac{3}{2}\rangle$	2.4
$\|541\frac{3}{2}\rangle \to \|\frac{1}{2}\rangle$	4.1	$\|624\frac{9}{2}\rangle \to \|\frac{7}{2}\rangle$	5.3
$\|402\frac{5}{2}\rangle \to \|\frac{3}{2}\rangle$	1.9	$\|633\frac{7}{2}\rangle \to \|\frac{5}{2}\rangle$	5.0
$\|411\frac{3}{2}\rangle \to \|\frac{1}{2}\rangle$	1.4	$\|642\frac{5}{2}\rangle \to \|\frac{3}{2}\rangle$	4.6
		$\|631\frac{3}{2}\rangle \to \|\frac{1}{2}\rangle$	7.8
$\langle 0'\|\mathbf{l}\cdot\mathbf{s}\|0'\rangle = 9$		$\langle 0'\|\mathbf{l}\cdot\mathbf{s}\|0'\rangle = 17$	
$\bar{E} = 13.8$ MeV, $\delta = 0.25$			

^{226}Ra

Proton transitions		Neutron transitions	
Transition	$E_{n'}$ (MeV)	Transition	$E_{n'}$ (MeV)
$\|523\frac{7}{2}\rangle \to \|\frac{5}{2}\rangle$	4.3	$\|624\frac{9}{2}\rangle \to \|\frac{7}{2}\rangle$	5.0
$\|514\frac{9}{2}\rangle \to \|\frac{7}{2}\rangle$	4.4	$\|615\frac{11}{2}\rangle \to \|\frac{9}{2}\rangle$	5.0
$\|505\frac{11}{2}\rangle \to \|\frac{9}{2}\rangle$	4.4	$\|606\frac{13}{2}\rangle \to \|\frac{11}{2}\rangle$	5.6
		$\|761\frac{3}{2}\rangle \to \|\frac{1}{2}\rangle$	4.3
$\langle 0'\|\mathbf{l}\cdot\mathbf{s}\|0'\rangle = 12$		$\langle 0'\|\mathbf{l}\cdot\mathbf{s}\|0'\rangle = 16$	
$\bar{E} = 13.0$ MeV, $\delta = 0.2$			

^{232}Th

Proton transitions		Neutron transitions	
Transition	$E_{n'}$ (MeV)	Transition	$E_{n'}$ (MeV)
$\|651\frac{3}{2}\rangle \to \|\frac{1}{2}\rangle$	4.5	$\|752\frac{5}{2}\rangle \to \|\frac{3}{2}\rangle$	4.1
$\|505\frac{11}{2}\rangle \to \|\frac{9}{2}\rangle$	4.2	$\|761\frac{3}{2}\rangle \to \|\frac{1}{2}\rangle$	4.0
$\|514\frac{9}{2}\rangle \to \|\frac{7}{2}\rangle$	4.0	$\|631\frac{3}{2}\rangle \to \|\frac{1}{2}\rangle$	1.0
$\|523\frac{7}{2}\rangle \to \|\frac{5}{2}\rangle$	3.7	$\|624\frac{9}{2}\rangle \to \|\frac{7}{2}\rangle$	5.0
		$\|615\frac{11}{2}\rangle \to \|\frac{9}{2}\rangle$	4.8
		$\|606\frac{13}{2}\rangle \to \|\frac{11}{2}\rangle$	5.4
$\langle 0'\|\mathbf{l}\cdot\mathbf{s}\|0'\rangle = 13$		$\langle 0'\|\mathbf{l}\cdot\mathbf{s}\|0'\rangle = 19$	
$\bar{E} = 12.9$ MeV, $\delta = 0.25$			

Appendix B: Evaluation of electronic matrix element

In this appendix, we present the details of the calculation of the electronic matrix element in Eq. (10). For

convenience, we use the spherical basis $(\mathbf{e}_+, \mathbf{e}_-, \mathbf{e}_0)$. The components of the vectors in this basis will be labeled by the $(+,-,0)$ subscripts. Due to spherical symmetry, Eq. (10) may be conveniently rewritten as

$$M = e^2 \left(\langle p_{1/2}| \frac{n_0}{r^2} |0_B\rangle + \langle p_{1/2}| \frac{(\mathbf{n}\times\boldsymbol{\alpha})_0}{r^2} |0_E\rangle \right) , \quad \text{(B1)}$$

where the wave functions $|0_B\rangle$ and $|0_E\rangle$ are defined by

$$|0_B\rangle \equiv \sum_n \frac{|n\rangle \langle n| \frac{(\mathbf{n}\times\boldsymbol{\alpha})_0}{r^2} |s_{1/2}\rangle}{E_{s_{1/2}0'} - E_{nn'}} , \quad \text{(B2a)}$$

$$|0_E\rangle \equiv \sum_n \frac{|n\rangle \langle n| \frac{n_0}{r^2} |s_{1/2}\rangle}{E_{s_{1/2}0'} - E_{nn'}} . \quad \text{(B2b)}$$

By construction, these wave functions obey the equations

$$(H_0 + E_{n'} - E_{s_{1/2}0'})|0_B\rangle = -\frac{(\mathbf{n}\times\boldsymbol{\alpha})_0}{r^2}|s_{1/2}\rangle , \quad \text{(B3a)}$$

$$(H_0 + E_{n'} - E_{s_{1/2}0'})|0_E\rangle = -\frac{n_0}{r^2}|s_{1/2}\rangle , \quad \text{(B3b)}$$

where H_0 is the unperturbed electronic Hamiltonian, $H_0|n\rangle = E_n|n\rangle$. In this appendix, we solve the equations (B3) for $|0_B\rangle$ and $|0_E\rangle$ and determine the values of the electronic matrix element (B1) for particular nuclear energies $E_{n'}$ tabulated in Appendix A. From this point on, without loss of generality, we set $E_{s_{1/2}0'} = 0$.

Equations (B3) may be solved in different ranges of the radial variable r. As will be demonstrated in Sect. B1, analytical solutions to Eqs. (B3) exist for $r \ll Z\alpha/E_{n'}$, i.e., in the region very close to the nucleus. However, the leading contribution to Eq. (B1) comes from distances beyond the vicinity of the nucleus. We will compute this contribution numerically in Sect. B2.

B1: Short-range contribution

At small distances from the nucleus, $r \ll a_B/Z$, the inter-electron interaction is negligible as compared to the Coulomb interaction of the electrons with the nucleus. Therefore, in this region, the electron unperturbed Hamiltonian is simply $H_0 = \boldsymbol{\alpha}\cdot\mathbf{p} + \beta m_e - Z\alpha/r$. Also, in this regime, the unperturbed $s_{1/2}$ and $p_{1/2}$ wave functions have the simple form (4). In this section, we will employ these approximate wave functions to determine the short-range contributions to the electronic matrix element (B1).

With the wave functions (4), the right-hand sides in Eqs. (B3) may be written as

$$\frac{(\mathbf{n}\times\boldsymbol{\alpha})_0}{r^2}|s_{1/2}\rangle = \frac{c_{s_{1/2}}}{r^{3-\gamma}} \sum_{\kappa=-1,2} \lambda_\mu^\kappa \begin{pmatrix} -Z\alpha\Omega_\mu^\kappa \\ i(1+\gamma)\Omega_\mu^{-\kappa} \end{pmatrix} , \quad \text{(B4a)}$$

$$\frac{n_0}{r^2}|s_{1/2}\rangle = \frac{c_{s_{1/2}}}{r^{3-\gamma}} \sum_{\kappa=-1,2} \chi_\mu^\kappa \begin{pmatrix} -(\gamma+1)\Omega_\mu^{-\kappa} \\ iZ\alpha\Omega_\mu^\kappa \end{pmatrix} , \quad \text{(B4b)}$$

where the coefficients λ_μ^κ and χ_μ^κ are defined via the algebraic equations $(\mathbf{n}\times\boldsymbol{\sigma})_0\Omega_\mu^1 = i(\lambda_\mu^{-1}\Omega_\mu^{-1} + \lambda_\mu^2\Omega_\mu^2)$ and $n_0\Omega_\mu^1 = \chi_\mu^{-1}\Omega_\mu^{-1} + \chi_\mu^2\Omega_\mu^2$, respectively. Explicitly, they are [54]: $\lambda_{1/2}^{-1} = 2/3$, $\lambda_{1/2}^2 = \sqrt{2}/3$ and $\chi_{1/2}^{-1} = -1/3$, $\chi_{1/2}^2 = \sqrt{2}/3$.

Equations (B4) suggest to look for the solutions to Eqs. (B3) in the form

$$|0_B\rangle = c_{s_{1/2}} \sum_{\kappa=-1,2} \lambda_\mu^\kappa \begin{pmatrix} f_B^\kappa(r)\Omega_\mu^\kappa \\ ig_B^\kappa(r)\Omega_\mu^{-\kappa} \end{pmatrix} , \quad \text{(B5a)}$$

$$|0_E\rangle = c_{s_{1/2}} \sum_{\kappa=-1,2} \chi_\mu^\kappa \begin{pmatrix} f_E^\kappa(r)\Omega_\mu^{-\kappa} \\ ig_E^\kappa(r)\Omega_\mu^\kappa \end{pmatrix} , \quad \text{(B5b)}$$

with some yet unknown radial functions f_B^κ, g_B^κ, f_E^κ and g_E^κ. Substituting the solutions (B5) into Eqs. (B3), we obtain the differential equations for these radial functions

$$\frac{df_B^\kappa}{dr} + \frac{1+\kappa}{r} f_B^\kappa + \left(E_{n'} - \frac{Z\alpha}{r}\right) g_B^\kappa = -\frac{1+\gamma}{r^{3-\gamma}} , \quad \text{(B6a)}$$

$$\frac{dg_B^\kappa}{dr} + \frac{1-\kappa}{r} g_B^\kappa - \left(E_{n'} - \frac{Z\alpha}{r}\right) f_B^\kappa = -\frac{Z\alpha}{r^{3-\gamma}} , \quad \text{(B6b)}$$

and

$$\frac{df_E^\kappa}{dr} + \frac{1-\kappa}{r} f_E^\kappa + \left(E_{n'} - \frac{Z\alpha}{r}\right) g_E^\kappa = -\frac{Z\alpha}{r^{3-\gamma}} , \quad \text{(B7a)}$$

$$\frac{dg_E^\kappa}{dr} + \frac{1+\kappa}{r} g_E^\kappa - \left(E_{n'} - \frac{Z\alpha}{r}\right) f_E^\kappa = -\frac{1+\gamma}{r^{3-\gamma}} , \quad \text{(B7b)}$$

where we have neglected the electron mass m_e in comparison with the nuclear energy $E_{n'}$.

In general, Eqs. (B6) and (B7) are hard to solve analytically. However, for small distances $r \ll Z\alpha/E_{n'}$, the nuclear energies in these equations may be discarded in comparison with the other terms. In this case, the solutions to Eqs. (B6) and (B7) may be written explicitly as

$$\begin{pmatrix} f_B^\kappa \\ g_B^\kappa \end{pmatrix} = \frac{r^{\gamma-2}}{2-2\gamma-\kappa^2} \begin{pmatrix} (1+\gamma)\,\kappa \\ -Z\alpha\,(\kappa-2) \end{pmatrix} , \quad \text{(B8a)}$$

$$\begin{pmatrix} f_E^\kappa \\ g_E^\kappa \end{pmatrix} = -\frac{r^{\gamma-2}}{2-2\gamma-\kappa^2} \begin{pmatrix} Z\alpha\,(2\gamma+\kappa) \\ (1+\gamma)\,(2\gamma-\kappa-2) \end{pmatrix} . \quad \text{(B8b)}$$

Substituting the solutions (B8) into Eq. (B1) and integrating over radial and angular coordinates, we obtain the short-range contribution to the electronic matrix element M

$$M^{(s)} = \frac{4e^2 c_{s_{1/2}} c_{p_{1/2}}}{3} \frac{(1-\gamma)^2}{2\gamma-1} I , \quad \text{(B9)}$$

where I is the integral over the radial variable,

$$I = \int_{R_0}^{R_1} dr\, r^{2\gamma-3} = \frac{R_0^{2\gamma-2} - R_1^{2\gamma-2}}{2(1-\gamma)} . \quad \text{(B10)}$$

The integration region here is from the nuclear radius R_0 to the quantity $R_1 = Z\alpha/(2E_{n'})$, where the obtained solutions (B8) are applicable. The superscript (s) signifies the short-range contribution to M.

The short-range contributions to the electronic factors $M_p^{(s)}$ and $M_n^{(s)}$ are presented in Table III. These short-range contributions are comparable to those found in Ref. [32].

B2: Numerical solution including short- and mid-range contributions

In section B1, we estimated the contribution to the electronic matrix element (B1) arising from the near-nucleus region. However, as will be demonstrated below, the dominant contribution to the quantity M comes from distances beyond the neighbourhood of the nucleus.

Note that for $r \gg R_2 = \max(1 \pm \kappa)/E_{n'}$, the terms proportional to $1/r$ in Eqs. (B6) and (B7) may be neglected in comparison with those proportional to $E_{n'}$. As a result, the solutions $f_{B,E}$ and $g_{B,E}$ for $r \gg R_2$ are approximately independent of κ. The sums over κ in the electronic matrix elements (B1), when carried out, will result in a factor $\mathbf{n}\cdot(\mathbf{n}\times\boldsymbol{\sigma}) = 0$. The vanishing of this long-range contribution was pointed out in Ref. [42]. Taking this into consideration, we will limit our attention only to the region $R_0 \le r \le qR_2$ where $q \gtrsim 1$.

Also, in this range, we have $r \ll a_B/Z^{1/3}$ so the electron screening of the Coulomb potential is negligible [44] and we may use the full charge number Z in Eqs. (B6) and (B7). Furthermore, the $s_{1/2}$ and $p_{1/2}$ radial wave functions are well approximated by (see, e.g., [44])

$$f_{s_{1/2}} = \frac{k_{s_{1/2}}}{r}\left[(-1+\gamma)J_{2\gamma}(x) - \frac{x}{2}J_{2\gamma-1}(x)\right], \quad \text{(B11a)}$$

$$f_{p_{1/2}} = \frac{k_{p_{1/2}}}{r}\left[(1+\gamma)J_{2\gamma}(x) - \frac{x}{2}J_{2\gamma-1}(x)\right], \quad \text{(B11b)}$$

$$g_{s_{1/2}} = \frac{k_{s_{1/2}}}{r}Z\alpha J_{2\gamma}(x), \quad \text{(B11c)}$$

$$g_{p_{1/2}} = \frac{k_{p_{1/2}}}{r}Z\alpha J_{2\gamma}(x), \quad \text{(B11d)}$$

where $J_\nu(x)$ is the Bessel function of the first kind, $k_{s,p_{1/2}} \equiv c_{s,p_{1/2}}\Gamma(2\gamma+1)\left(\frac{a_B}{2Z}\right)^\gamma$ and $x \equiv \sqrt{8Zr/a_B}$.

The radial wave functions (B11) are to be substituted into the right-hand sides of Eqs. (B6) and (B7), which now read

$$\frac{df_B^\kappa}{dr} + \frac{1+\kappa}{r}f_B^\kappa + \left(E_{n'} - \frac{Z\alpha}{r}\right)g_B^\kappa = \frac{f_{s_{1/2}}}{r^2}, \quad \text{(B12a)}$$

$$\frac{dg_B^\kappa}{dr} + \frac{1-\kappa}{r}g_B^\kappa - \left(E_{n'} - \frac{Z\alpha}{r}\right)f_B^\kappa = -\frac{g_{s_{1/2}}}{r^2}, \quad \text{(B12b)}$$

and

$$\frac{df_E^\kappa}{dr} + \frac{1-\kappa}{r}f_E^\kappa + \left(E_{n'} - \frac{Z\alpha}{r}\right)g_E^\kappa = -\frac{g_{s_{1/2}}}{r^2}, \quad \text{(B13a)}$$

$$\frac{dg_E^\kappa}{dr} + \frac{1+\kappa}{r}g_E^\kappa - \left(E_{n'} - \frac{Z\alpha}{r}\right)f_E^\kappa = \frac{f_{s_{1/2}}}{r^2}. \quad \text{(B13b)}$$

Note that for $r \ll a_B/Z$, Eqs. (B11) reduce to the short-range asymptotic form, so the solutions (B8) are already included in those of Eqs. (B12) and (B13). As a result, for $r \ll a_B/Z$, the numerical solutions to Eqs. (B12) and (B13) must reduce to Eqs. (B8). We thus enforce the boundary conditions by requiring that the values of the numerical solutions to Eqs. (B12) and (B13) at $r = R_0$ are

$$\begin{pmatrix} f_B^\kappa \\ g_B^\kappa \end{pmatrix} = \frac{R_0^{\gamma-2}}{2-2\gamma-\kappa^2}\begin{pmatrix} (1+\gamma)\kappa \\ -Z\alpha(\kappa-2) \end{pmatrix}, \quad \text{(B14a)}$$

$$\begin{pmatrix} f_E^\kappa \\ g_E^\kappa \end{pmatrix} = -\frac{R_0^{\gamma-2}}{2-2\gamma-\kappa^2}\begin{pmatrix} Z\alpha(2\gamma+\kappa) \\ (1+\gamma)(2\gamma-\kappa-2) \end{pmatrix}. \quad \text{(B14b)}$$

		M_p $\left(\frac{10^{-2}}{\text{fm}^3}\right)$	M_n $\left(\frac{10^{-2}}{\text{fm}^3}\right)$	$M(\bar{E})$ $\left(\frac{10^{-3}}{\text{fm}^3}\right)$	$M_p^{(s)}$ $\left(\frac{10^{-3}}{\text{fm}^3}\right)$	$M_n^{(s)}$ $\left(\frac{10^{-3}}{\text{fm}^3}\right)$
Spherical	^{138}Ba	3.76	3.62	2.00	0.06	0.00
	^{206}Pb	3.81	7.56	1.33	0.62	0.78
	^{208}Pb	3.80	2.77	1.34	0.62	0.26
Deformed	^{172}Yb	7.76	8.68	1.89	0.50	0.51
	^{174}Yb	7.74	13.2	1.90	0.50	0.79
	^{176}Yb	7.72	11.1	1.91	0.49	0.66
	^{178}Hf	20.7	10.2	1.86	1.30	0.62
	^{180}Hf	20.6	11.5	1.85	1.30	0.68
	^{226}Ra	3.83	4.21	0.67	1.23	1.28
	^{232}Th	5.26	12.0	0.41	2.03	3.31

Table III: Electronic matrix elements M_p, M_n and $M(\bar{E})$ for several atoms of interest. The values of the matrix elements M are given relative to the normalization constant $c_{s_{1/2}}c_{p_{1/2}}$. The superscript (s) labels the short-range contributions presented here for comparison.

With the above boundary conditions, Eqs. (B12) and (B13) may be solved numerically in the region $R_0 \le r \le qR_2$. In Fig. 1, we show that the values of electronic matrix elements are not sensitive to a particular choice of the parameter q subject to the constraint $q \gtrsim 25$. The values of the nuclear energies needed for computation are taken from the tables presented in the Sect. B1. The obtained solutions $f_{B,E}^\kappa$ and $g_{B,E}^\kappa$ are then integrated with the $p_{1/2}$ wave function with radial parts as given in Eqs. (B11b) and (B11d). The resulting numerical values of the electronic factors M_p, M_n and $M(\bar{E})$ are presented in Table. III. In this table, we give also the short-range

contributions to these coefficients labeled by the superscript (s). As is seen from this table, the mid-range contribution dominates over the short-range one.

As an illustration, we present also a plot in Figure 1, which shows the dependence of the electronic matrix element $M(5\,\mathrm{MeV})$, corresponding to the 5-MeV neutron spin-flip transition in ^{232}Th on the upper limit qR_2 of the radial integrals. Clearly, near-nucleus contributions are negligible in comparison with mid-range ones. It is also clear that long-range contributions vanish and the result saturates as we increase the cut-off.

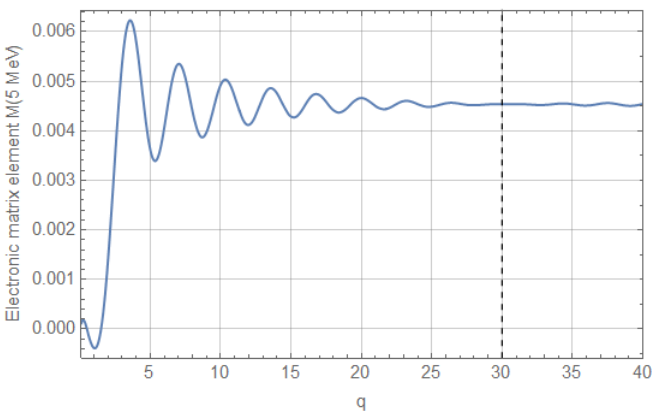

Figure 1: Dependence of the electronic matrix element $M(5\,\mathrm{MeV})$ corresponding to the 5-MeV neutron spin-flip transition in ^{232}Th on the upper limit qR_2 of the radial integrals. The dash line shows the actual cut-off employed in the numerical computation.

[1] N. Cabibbo, Phys. Rev. Lett. **10**, 531 (1963).
[2] M. Kobayashi and T. Maskawa, Prog. Theor. Phys. **49**, 652 (1973).
[3] R. D. Peccei and H. R. Quinn, Phys. Rev. Lett. **38**, 1440 (1977).
[4] S. Weinberg, Phys. Rev. Lett. **40**, 223 (1978).
[5] F. Wilczek, Phys. Rev. Lett. **40**, 279 (1978).
[6] N. Yamanaka, B. Sahoo, N. Yoshinaga, T. Sato, K. Asahi, and B. Das, Eur. Phys. J. A **53**, 54 (2017).
[7] T. E. Chupp, P. Fierlinger, M. J. Ramsey-Musolf, and J. T. Singh, Rev. Mod. Phys. **91**, 015001 (2019).
[8] W. C. Griffith, M. D. Swallows, T. H. Loftus, M. V. Romalis, B. R. Heckel, and E. N. Fortson, Phys. Rev. Lett. **102**, 101601 (2009).
[9] C. A. Baker, D. D. Doyle, P. Geltenbort, K. Green, M. G. D. van der Grinten, P. G. Harris, P. Iaydjiev, S. N. Ivanov, D. J. R. May, J. M. Pendlebury, et al., Phys. Rev. Lett. **97**, 131801 (2006).
[10] J. J. Hudson, D. M. Kara, I. Smallman, B. E. Sauer, M. R. Tarbutt, and E. A. Hinds, Nature **473**, 493 (2011).
[11] J. Baron, W. C. Campbell, D. DeMille, J. M. Doyle, G. Gabrielse, Y. V. Gurevich, P. W. Hess, N. R. Hutzler, E. Kirilov, I. Kozyryev, et al., Science **343**, 269 (2014).
[12] R. H. Parker, M. R. Dietrich, M. R. Kalita, N. D. Lemke, K. G. Bailey, M. Bishof, J. P. Greene, R. J. Holt, W. Korsch, Z.-T. Lu, et al., Phys. Rev. Lett. **114**, 233002 (2015).
[13] J. M. Pendlebury, S. Afach, N. J. Ayres, C. A. Baker, G. Ban, G. Bison, K. Bodek, M. Burghoff, P. Geltenbort, K. Green, et al., Phys. Rev. D **92**, 092003 (2015).
[14] B. Graner, Y. Chen, E. G. Lindahl, and B. R. Heckel, Phys. Rev. Lett. **116**, 161601 (2016).
[15] G. E. Harrison, P. G. H. Sandars, and S. J. Wright, Phys. Rev. Lett. **23**, 274 (1969).
[16] E. A. Hinds and P. G. H. Sandars, Phys. Rev. A **21**, 480 (1980).
[17] D. A. Wilkening, N. F. Ramsey, and D. J. Larson, Phys. Rev. A **29**, 425 (1984).
[18] D. Schropp, D. Cho, T. Vold, and E. A. Hinds, Phys. Rev. Lett. **59**, 991 (1987).
[19] D. Cho, K. Sangster, and E. A. Hinds, Phys. Rev. A **44**, 2783 (1991).
[20] T. G. Vold, F. J. Raab, B. Heckel, and E. N. Fortson, Phys. Rev. Lett. **52**, 2229 (1984).
[21] T. E. Chupp, R. J. Hoare, R. L. Walsworth, and B. Wu, Phys. Rev. Lett. **72**, 2363 (1994).
[22] R. E. Stoner, M. A. Rosenberry, J. T. Wright, T. E. Chupp, E. R. Oteiza, and R. L. Walsworth, Phys. Rev. Lett. **77**, 3971 (1996).
[23] D. Bear, T. E. Chupp, K. Cooper, S. DeDeo, M. Rosenberry, R. E. Stoner, and R. L. Walsworth, Phys. Rev. A **57**, 5006 (1998).
[24] M. A. Rosenberry and T. E. Chupp, Phys. Rev. Lett. **86**, 22 (2001).
[25] M. V. Romalis, W. C. Griffith, J. P. Jacobs, and E. N. Fortson, Phys. Rev. Lett. **86**, 2505 (2001).
[26] M. Bishof, R. H. Parker, K. G. Bailey, J. P. Greene, R. J. Holt, M. R. Kalita, W. Korsch, N. D. Lemke, Z.-T. Lu, P. Mueller, et al., Phys. Rev. C **94**, 025501 (2016).
[27] H. Loh, K. C. Cossel, M. C. Grau, K.-K. Ni, E. R. Meyer, J. L. Bohn, J. Ye, and E. A. Cornell, Science **342**, 1220 (2013).
[28] S. Eckel, P. Hamilton, E. Kirilov, H. W. Smith, and D. DeMille, Phys. Rev. A **87**, 052130 (2013).
[29] W. B. Cairncross, D. N. Gresh, M. Grau, K. C. Cossel, T. S. Roussy, Y. Ni, Y. Zhou, J. Ye, and E. A. Cornell, Phys. Rev. Lett. **119**, 153001 (2017).
[30] P. Aggarwal, H. L. Bethlem, A. Borschevsky, M. Denis, K. Esajas, P. A. Haase, Y. Hao, S. Hoekstra, K. Jungmann, T. B. Meijknecht, et al., Eur. Phys. J. D **72**, 197 (2018).
[31] V. Andreev, D. G. Ang, D. DeMille, J. M. Doyle, G. Gabrielse, J. Haefner, N. R. Hutzler, Z. Lasner, C. Meisenhelder, B. R. O'Leary, et al. (ACME Collaboration), Nature **562**, 355 (2018).
[32] V. V. Flambaum, M. Pospelov, A. Ritz, and Y. V. Stadnik, arXiv:1912.13129 (2019).
[33] L. I. Schiff, Phys. Rev. **132**, 2194 (1963).
[34] O. Sushkov, V. Flambaum, and I. Khriplovich, Zh. Eksp. Teor. Fiz **87**, 1521 (1984).
[35] V. Flambaum, I. Khriplovich, and O. Sushkov, Nucl. Phys. A **449**, 750 (1986).
[36] V. Flambaum, Phys. Lett. B **320**, 211 (1994).
[37] V. Dzuba, V. Flambaum, P. Silvestrov, and O. Sushkov, Phys. Lett. A **118**, 177 (1986).
[38] V. V. Flambaum, Phys. Rev. A **98**, 043408 (2018).
[39] H. B. T. Tan, V. V. Flambaum, and I. B. Samsonov,

Phys. Rev. A **99**, 013430 (2019).
[40] V. V. Flambaum and I. B. Samsonov, Phys. Rev. A **98**, 053437 (2018).
[41] V. Flambaum and I. Samsonov, Phys. Rev. Res. **2**, 023042 (2020).
[42] V. V. Flambaum, J. S. M. Ginges, and G. Mititelu, arXiv:nucl-th/0010100 (2000).
[43] V. Flambaum and I. Khriplovich, Zh. Eksp. Theor. Fiz **89**, 1505 (1985).
[44] I. B. Khriplovich, *Parity nonconservation in atomic phenomena* (Gordon and Breach Science Publishers, 1991).
[45] S. Nilsson, Mat.-Fys. Medd. K. Dan. Vidensk. Selsk. **29**, 1–69 (1955).
[46] A. Bohr and B. R. Mottelson, *Nuclear Structure*, vol. 2 (World Scientific, Singapore, 1998).
[47] T. Fleig and M. Jung, J. High Energy Phys. **2018**, 12 (2018).
[48] R. Crewther, P. Di Vecchia, G. Veneziano, and E. Witten, Phys. Lett. B **88**, 123 (1979).
[49] M. Pospelov and A. Ritz, Ann. Phys. **318**, 119 (2005), special Issue.
[50] V. V. Flambaum, D. DeMille, and M. G. Kozlov, Phys. Rev. Lett. **113**, 103003 (2014).
[51] J. de Vries, E. Mereghetti, and A. Walker-Loud, Phys. Rev. C **92**, 045201 (2015).
[52] J. Bsaisou, J. de Vries, C. Hanhart, S. Liebig, U.-G. Meißner, D. Minossi, A. Nogga, and A. Wirzba, J. High Energy Phys. **2015**, 104 (2015).
[53] H. Loh, K. C. Cossel, M. C. Grau, K.-K. Ni, E. R. Meyer, J. L. Bohn, J. Ye, and E. A. Cornell, Science **342**, 1220 (2013).
[54] R. Szmytkowski, J. Math. Chem. **42**, 397 (2007).
[55] A. V. Nefiodov, L. N. Labzowsky, G. Plunien, and G. Soff, Phys. Lett. A **222**, 227 (1996).
[56] G. Plunien and G. Soff, Phys. Rev. A **51**, 1119 (1995).